Japanese Journal of Applied Physics

REGULAR PAPER

Dynamically tunable ultralong photonic nanojets by a curved surface truncated dielectric microcylinder

To cite this article: Yi Xing *et al* 2022 *Jpn. J. Appl. Phys.* **61** 022002

Japanese Journal of Applied Physics **61**, 022002 (2022) **REGULAR PAPER**
https://doi.org/10.35848/1347-4065/ac404f

Dynamically tunable ultralong photonic nanojets by a curved surface truncated dielectric microcylinder

Yi Xing[1,2], Fengfeng Shu[1*], Huaming Xing[1], and Yihui Wu[1*]

[1]*State Key Laboratory of Applied Optics, Changchun Institute of Optics, Fine Mechanics and Physics, Chinese Academy of Science, Changchun 130033, People's Republic of China*
[2]*University of Chinese Academy of Sciences, Beijing 100039, People's Republic of China*

[*]E-mail: sff@ciomp.ac.cn; yihuiwu@ciomp.ac.cn

Received November 8, 2021; accepted December 5, 2021; published online January 24, 2022

As for microparticles (microspheres or microcylinders) that form photonic nanojets (PNJs) in the near field, a curved truncated dielectric microcylinder structure (CSTDM) is investigated by the finite element method which can form ultralong PNJs with the longest effective length: 209.49 λ. Changing parameter *h* of the structure can realize long dynamic range tuning of the effective length of the PNJ. The effective length varies quasi-periodically with *h*; the law of the variation of main indicators of the microcylinder is further discussed, such as the effective length, the working distance, peak electric field intensity, and full width at half height.

1. Introduction

Photonic nanojets (PNJs) are a high-intensity narrow focus in the shadow side of microparticles illuminated by plane waves. This characteristic of microparticles was reported by Owen et al. in 1981,[1)] Benincasa et al. proved that this phenomenon exists even under non-resonant conditions.[2)] Chen et al. showed the formation of PNJs of microcylinders by numerically calculation based on Maxwell's equations, and introduce the term 'PNJ'.[3)] Li et al. used the rigorous analytical solution obtained by solving Maxwell's equations with the Mie theory to explain the backscattering of the dielectric sphere.[4)] Due to the characteristics of PNJs high-intensity super-resolution focusing and easy assembly,[5)] it is widely used, including in photolithography,[6–8)] microsphere-assisted microscopy,[9)] laser material processing and dry laser cleaning,[10,11)] high-density optical data-storage disks[12)] Although many studies have achieved a series of pioneering results in compressing the beam waist,[13–17)] one of the shortcomings of PNJs is that the focal point is near the surface of the microparticles. The short effective length and working distance greatly limit its applications. In recent years, many studies have been put forward to improve these drawbacks. Most of these studies start from three aspects: first, changing the internal refractive distribution of the microparticles. S. C. Kong et al. proposed gradient index microspheres and the simulation realized a PNJ with an effective length of 20 λ (λ is the illumination wavelength);[18)] Shen et al. reported a 22 λ ultralong PNJ by a two-layer microsphere structure with different refractive indexes,[19)] he also indicated that the key point of obtaining a long PNJ is to engineer microspheres so that the power flow near the focal point is essentially parallel so as to have a small angular deviation. The second was to control the refractive index contrast. G. Gu. et al. presented a liquid-filled hollow microcylinder (LFHM) under liquid immersion conditions with an effective length of more than 100 λ;[20)] Wu et al. reported an effective length of 57 λ by liquid-immersed cores Shell microspheres;[21)] Third, engineer the structure of microparticles. Paul et al. reported a truncated multilayer microsphere (TMLM) structure, and the results realized a PNJ with an effective length of 138 μm (172 λ) and a working distance of 26 μm (32 λ);[22)] Zhou et al. proposed a negative prism microsphere structure, the effective length and working distance reached 120.4 λ and 52 λ.[23)] However, these methods have their inevitable disadvantages, for instance, short effective length and difficulty in manufacture or use.

2. Design and principle

In this letter, we propose a curved surface truncated microcylinder structure composed of a single medium to realize an ultralong nanojet, the maximum effective length can reach 209.49 λ. The effect of truncated microparticles has been discussed, the curved surface truncated type has a great influence on elongating the PNJ. Especially, the change of the *h* parameter will cause a quasi-periodic change of PNJ's effective length. In addition, an obvious advantage of this structure is formed by a single material. We also design an structure for ease of use. We believe this structure has potential applications in many aspects, such as laser direct writing, beam control, and so on.

The numerical analysis model is shown in Fig. 1. It is formed by one microcylinder (the right in Fig. 1) to cut off another microcylinder (the left in Fig. 1) with the same refractive index and this transparent structure is considered as a 2D structure. The key point parameter *h* refers to the distance between the two sphere centers (that is, the distance from the front surface of the truncated microcylinder to the shadow side along the light transmission direction). r, n_1 are the radius and the refractive index of the truncated microcylinder (fused silica material) and n_2 is the refractive index of the environment (air): $n_1 = 1.4696$, $n_2 = 1.0$. I_{max} is the peak intensity of the PNJ focal point, the effective length L is the distance from the peak power I_{max} drops to $1/e$ of I_{max}. FWHM is the full width at half maximum of the PNJ, WD is the working distance which from the shadow side to the peak intensity. We used the finite element method based on Mie theory to calculate the electric field distribution of the curved truncated dielectric microcylinder structure (CSTDM). The illumination wave is a *z*-axis polarized plane wave ($\lambda = 405$ nm) propagating along the *y*-axis with an initial amplitude of 1 arbitrary unit (a.u.). The model is surrounded by a perfectly matched layer (PML). The mesh of CSTDM is 10 nm ($\frac{2}{81}\lambda$), the background mesh is 30 nm ($\frac{2}{27}\lambda$) to ensure the convergence of the mesh.

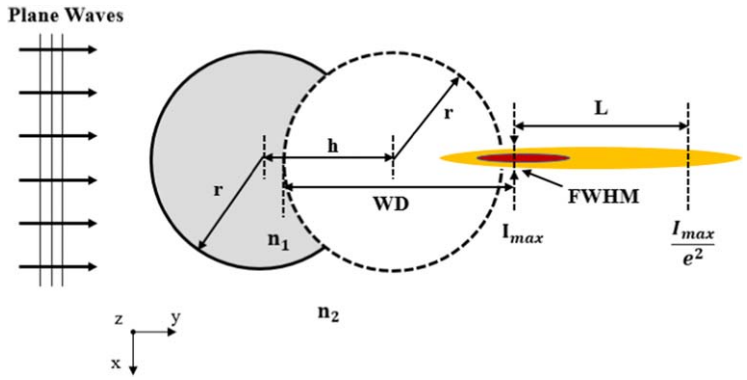

Fig. 1. (Color online) Schematic diagram of a structure of CSTDM used in the simulation.

We combined the Poynting vectors (in Fig. 2) to analyze the cause of the formation of ultralong PNJs in CSTDM. A single dielectric microcylinder [Fig. 2(a)] will form a short PNJ for that the rapid focus at the focal point will result in rapid divergence.[19] In order to achieve the purpose of an elongating PNJ, we start in two ways: first, we change the surface shape of the second interface, as shown in Fig. 2(b). As the second surface of the traditional microcylinder is convex, which has a converging effect on the outgoing beam. Changing it to a concave surface can slow down the convergence speed of the microcylinder at the focal point, and it will inevitably slow down its divergence speed to stretched out PNJ. Second, we shorten the optical path of the beam in the microcylinder (use the method of truncating the microcylinder), as shown in Fig. 2(c), which can weaken the convergent ability of the microcylinder to the beam and further elongate the PNJ.

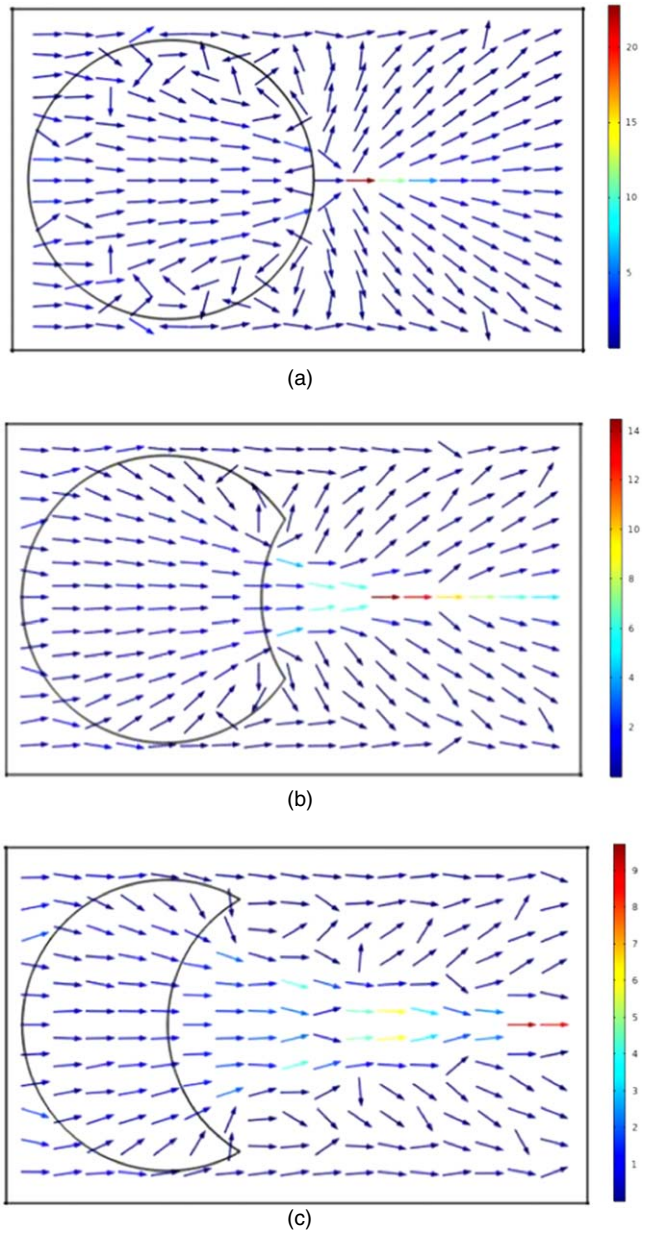

Fig. 2. (Color online) Poynting vectors plots of (a) a single microcylinder (b) CSTDM with $r = 4.5$ μm, $h = 7.5$ μm (c) CSTDM with $r = 4.5$ μm, $h = 4.5$ μm.

3. Simulation results and discussion

Figure 3 shows the electric field intensity of the PNJ

When $r = 4.5$ μm, $h = 8.8$ μm, 2.0 μm, 1.4 μm. By comparing Figs. 3(a) and 3(b), It can be initially found changing the second surface to a concave surface makes the outgoing beam closer to parallel near the focal point; as the decrease of h (the cut-off distance is larger), the optical path of the beam inside microcylinder is gradually reduced which weakens its converging ability to the beam and makes the PNJ relatively divergent. Thus, the effective length of the PNJ gradually becomes larger, especially when $h = 1.4$ μm, L is 209.49 λ, thus, the PNJ is further elongated. This is consistent with the optical explanation above.

We gradually reduce the h parameter from 9 μm to 0.8 μm to further analyze the change of L with an interval of 0.1 μm. Plot the changes of related physical quantities in Fig. 4. From Fig. 4(a), we find that as h gradually decreases, the overall trend of the L is rising exponentially, and WD gradually increases as h decreases. In addition, an interesting phenomenon is that L has a quasi-periodic change that initially goes up and then goes down as h decreases. In one cycle, there will be a periodic dramatic change with a small variety of h, the period is about 1.2 μm (2.96 λ). In the next paragraph, we will discuss the causes of this periodicity in detail. At the same time, Fig. 4(b) shows that I_{max} of the PNJ gradually goes down as h decreases. Because as L increases, the compression of the PNJ is weakened, the energy of the PNJ further diverges in the axial direction. On the other hand, it proves that we can make a PNJ relatively divergent by reducing h, and then get an ultralong PNJ. In addition, the FWHM gradually increases as h decreases, its value varies in

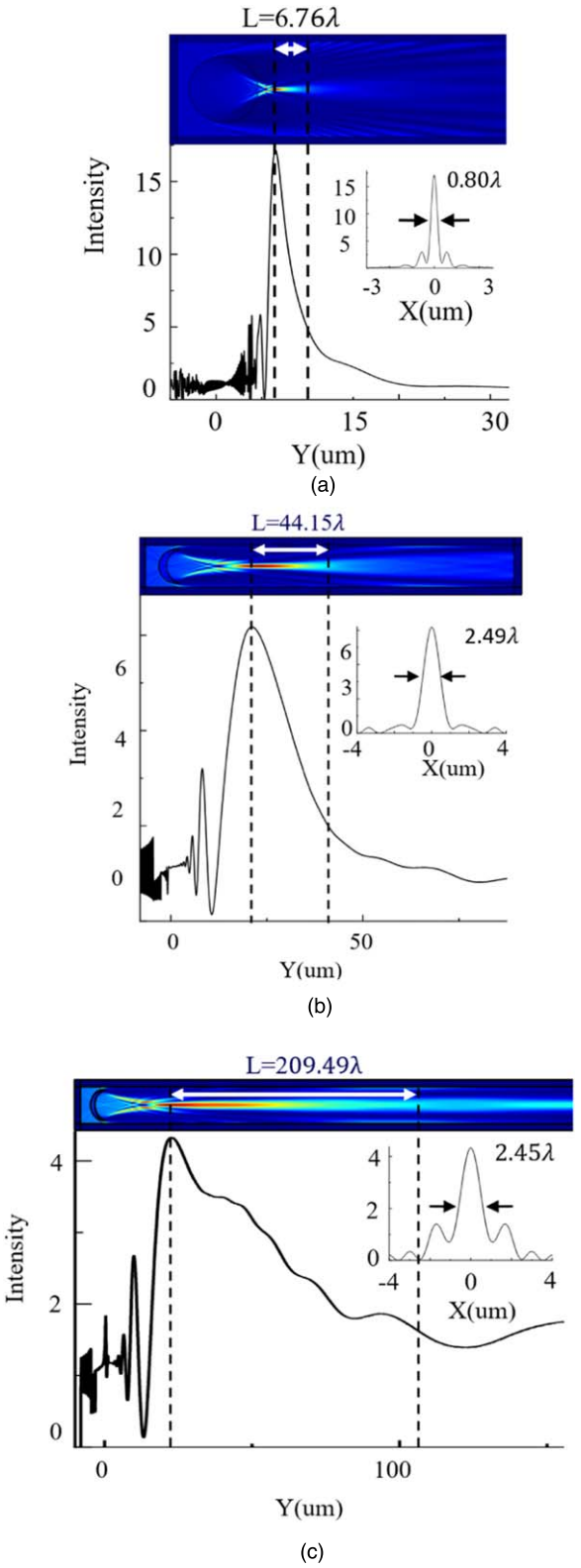

Fig. 3. (Color online) Intensity distribution of CSTDM of $r = 4.5$ μm. (a) $h = 8.8$ μm. (b) $h = 2.0$ μm. (c) $h = 1.4$ μm.

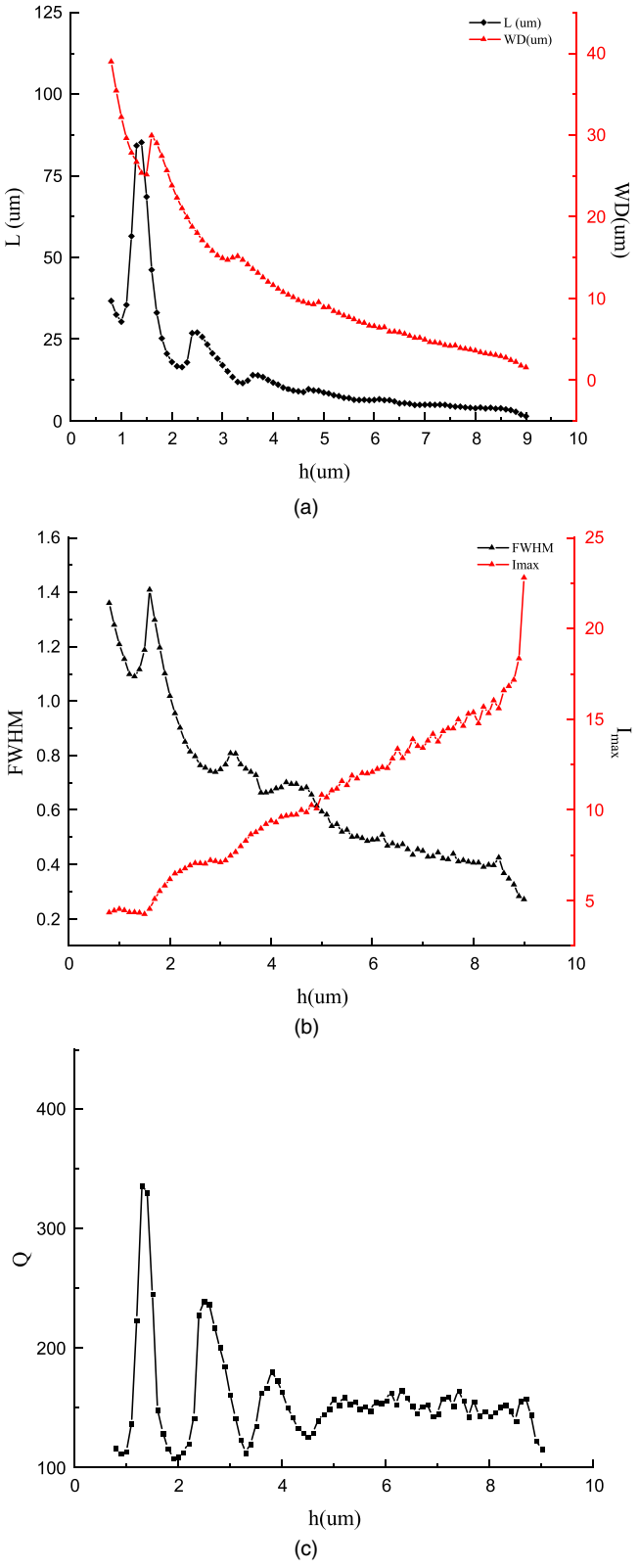

Fig. 4. (Color online) Key parameters of the PNJ as functions of h. when of $r = 4.5$ μm. (a) The effective length L and working distance WD as a function of h. (b) PNJ waist FWHM and peak intensity of PNJ I_{max} as a function of h. (c) PNJ quality criterion Q as a function of h.

a wide dynamic range from 248 nm to 1.628 μm. The energy will not only diverge along the optical axis, but the lateral energy also diverges along with the PNJ becoming longer. Therefore, the value of FWHM will inevitably increase. We believe that there is a compromise between ultralong PNJ and narrow FWHM. In order to better represent the characteristics of the PNJ, S. C. Kong et al. introduced the quality criterion Q:[17)]

$$Q = \frac{I_{\max} \cdot L}{\mathrm{FWHM}}$$

Figure 4(c) shows the Q factor as a function of the h parameter. When $h = 1.2$ μm, the Q factor has a maximum value, this means that the structure of this parameter has a

better compromise between longer effective length, stronger peak intensity, and narrower FWHM. One can dynamically adjust the effective length of the PNJ by adjusting the size of the h parameter according to the Q value.

In this section, we will further qualitatively discuss the cause of the periodic variation of the effective length L with h. Note that as h changes, the two quantities change accordingly, as shown in Fig. 5, one variable is the area of the long and narrow curved parts A and C on both sides. As h decreases, they will become smaller (the curvature does not change). It can be known through a simple geometric optics analysis (as shown in Fig. 6), the beam passes through areas A and C (red lines on both sides) converges closer to the exit surface, the convergence effect of area A, C on the light spot is much stronger than that of area B, it has a more obvious compression effect on the light spot. In other words, it has an inhibitory effect on extending the effective length. The other variable is the thickness h of the approximate rectangular area B in the middle, from the perspective of geometric optics analysis, the beam passes through area B (middle red line), and the beam is more likely to converge at a distance. Therefore, this area has a more obvious effect on extending the effective length.

We explore the influence of the two regions on L separately. First we choose CSTDM with $h = 2.0$ μm, using cut line $x = \pm L_x$ (two dashed line 1, 2 in Fig. 5). Reduce the area of A and C gradually, that is, reduce the inhibitory effect of the two sides on L to observe the change law of the effective length L. As shown in Fig. 7, L decreases with the increase of L_x, and the decreasing trend is similar to an exponential decrease. This means that the smaller the area at both sides, the longer the L elongated. This also has enlightenment for us to further extend the effective length L.

Next, we discuss the influence of the middle area B on L. We use the cut line of $x = \pm 3.5$ μm to cut off the narrow areas on both sides to make h a unique variable. The statistical change of L with h is shown in Fig. 8, we can see L changes periodically with h which means that the periodic change of h in Fig. 4(a) is related to the contribution of area B. However, the period here is not completely consistent with the period in Fig. 4. We think this is because when the two ends are not cut off, the converging effect of the two ends on the light spot increases as h decreases. All in all, it is the changes of area A, C and area B that together contribute to the change of the curve in Fig. 4(a) and the periodicity is mainly because of the contribution of area B.

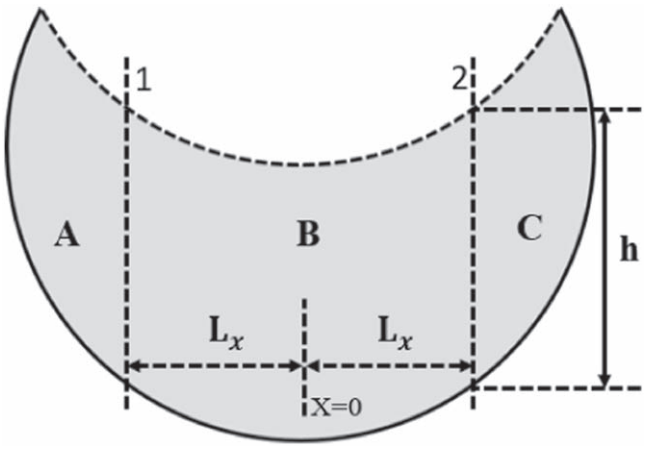

Fig. 5. Schematic diagram of the structure.

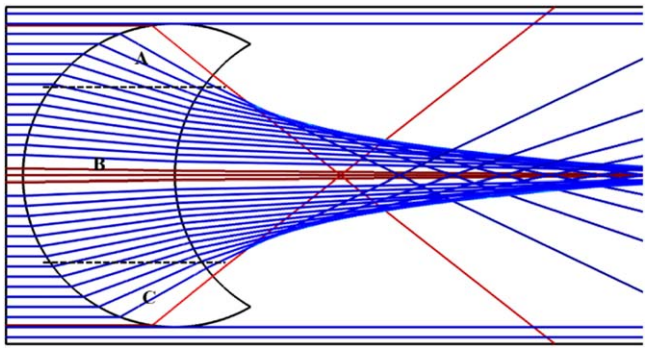

Fig. 6. (Color online) Optical tracing of CSTDM.

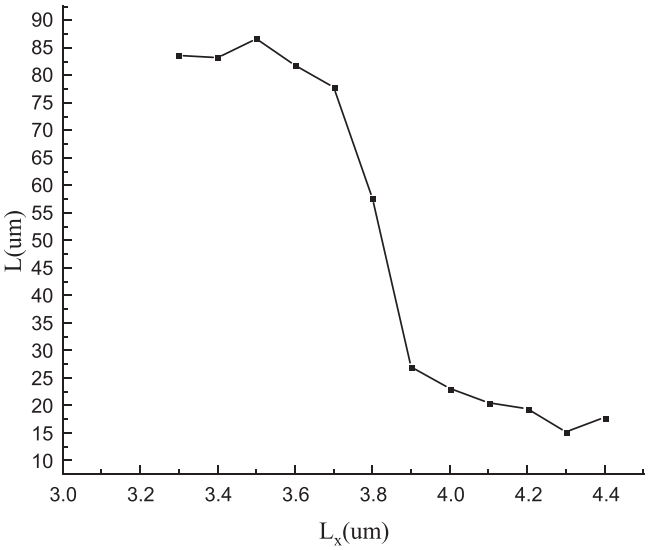

Fig. 7. The change curve of L with L_x.

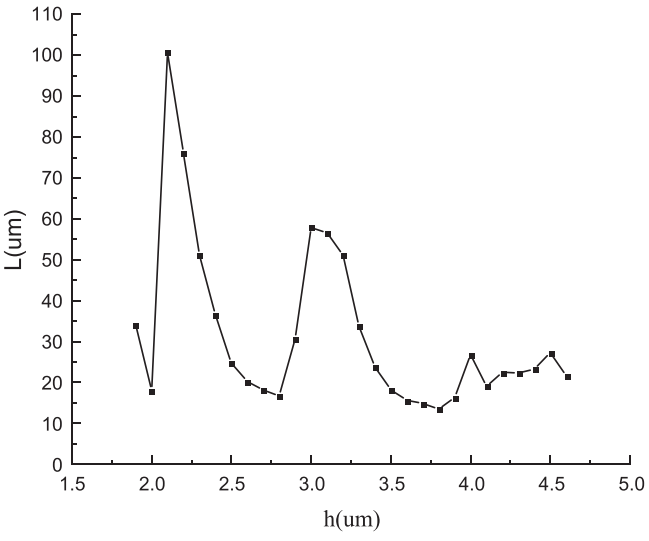

Fig. 8. The change curve of L with h.

Furthermore, in order to facilitate the use, we provide an easy-to-use structure, as shown in the dashed box in Fig. 9. Choose structure parameters as $r = 4.5$ μm, $h = 3.3$ μm, and flat the height of 0.1 μm at the bottom so that the device is easier to place on the supporting platform or samples. Through numerical analysis, as shown in Fig. 9, it is found

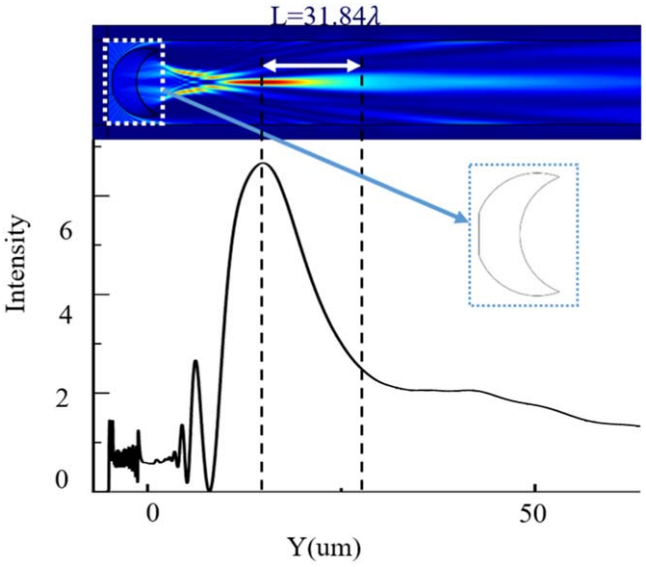

Fig. 9. (Color online) Intensity distribution of the CSTDM with $r = 4.5$ μm, $h = 3.3$ μm. The blue dotted line is a schematic diagram of the structure.

that the parameter value of the effective length and FWHM is slightly increased compared with the result of our initial design structure, but it is easier to place and use.

4. Conclusion

In summary, this paper proposes a CSTDM structure to obtain an ultralong effective length of PNJ, which can be up to 209.49 λ. At the same time, the study found that dynamic tuning of the PNJ effective length and other parameters can be achieved by adjusting the h parameter of the CSTDM and the law that the effective length L changes quasi-periodically with h. We believe that these findings have great potential to further promote the applications of the PNJ.

Acknowledgments

This work is supported by the National Key Research and Development program of China (No.2018YFF01013202).

1) J. F. Owen, R. K. Chang, and P. W. Barber, Opt. Lett. **6**, 540 (1981).
2) D. S. Benincasa, P. W. Barber, J. Z. Zhang, W. F. Hsieh, and R. K. Chang, Appl. Opt. **26**, 1348 (1987).
3) Z. Chen, A. Taflove, and V. Backman, Opt.Express. **12**, 1214 (2004).
4) X. Li, Z. Chen, A. Taflove, and V. Backman, Opt. Express **13**, 526 (2005).
5) X. Liang, R. Dong, and J. C. Ho, Adv. Mater. Technol. **4**, 1800541 (2019).
6) W. Wu, A. Katsnelson, O. G. Memis, and H. Mohseni, Nanotechnology **18**, 485302 (2007).
7) A. Bonakdar, M. Rezaei, E. Dexheimer, and H. Mohseni, Nanotechnology **27**, 035301 (2015).
8) A. Bonakdar, M. Rezaei, R. Brown, V. Fathipour, E. Dexheimer, S. J. Jang, and H. Mohseni, Opt. Lett. **40**, 2537 (2015).
9) Z. Wang, W. Guo, L. Li, B. Luk'Yanchuk, A. Khan, Z. Liu, Z. C. Chen, and M. Hong, Nat. Commun. **2**, 218 (2011).
10) Y. F. Lu, L. Zhang, W. D. Song, Y. W. Zheng, and B. S. Luk'Yanchuk, J. Exp. Theoret. Phys. Lett. **72**, 457 (2000).
11) E. Mcleod and C. B. Arnold, Nat. Nanotechnol. **3**, 413 (2008).
12) S. C. Kong, A. V. Sahakian, A. Heifetz, A. Taflove, and V. Backman, Appl. Phys. Lett. **92**, 211102 (2008).
13) H. Xing, W. Zhou, and Y. Wu, Opt. Lett. **43**, 4292 (2018).
14) B. Yan, L. Yue, and Z. Wang, Opt. Commun. **370**, 140 (2016).
15) L. Yue, B. Yan, J. N. Monks, Z. Wang, N. T. Tung, V. D. Lam, O. Minin, and I. Minin, J. Phys. D **50**, 175102 (2017).
16) Z. Zhen, Y. Huang, Y. Feng, Y. Shen, and Z. Li, Opt. Express **27**, 9178 (2019).
17) S. Zhou and T. Zhou, Appl. Phys. Express **13**, 042010 (2020).
18) S. C. Kong, A. Taflove, and V. Backman, Opt. Express **17**, 3722 (2009).
19) Y. Shen, L. V. Wang, and J. T. Shen, Opt. Lett. **39**, 4120 (2014).
20) G. Gu, R. Zhou, Z. Chen, H. Xu, G. Cai, Z. Cai, and M. Hong, Opt. Lett. **40**, 625 (2015).
21) P. Wu, J. Li, K. Wei, and W. Yue, Appl. Phys. Express **8**, 112001 (2015).
22) P. K. Upputuri, M. Krisnan, and M. Pramanik, J. Biomed. Opt. **22**, 045001 (2016).
23) Y. Zhou, R. Ji, J. Teng, and M. Hong, Eng. Res. Express **2**, 015044 (2020).